Polymer Chemistry

ROYAL SOCIETY OF CHEMISTRY

PAPER

View Article Online
View Journal | View Issue

Cite this: *Polym. Chem.*, 2023, **14**, 4101

Thermoresponsive behaviour of poly(*N*,*N*-diethylacrylamide) in aqueous two-phase systems†

Niamh Bayliss,[a] Gokhan Yilmaz,[b] Alexander Plucinski,[a] C. Remzi Becer [b] and Bernhard V. K. J. Schmidt *[a]

Received 23rd June 2023,
Accepted 9th August 2023

DOI: 10.1039/d3py00734k

rsc.li/polymers

Aqueous two-phase systems (ATPS) have been in the focus of polymer chemistry in recent years, mainly due to their biocompatibility and various applications in biomaterials and biology. In the present contribution, the ATPS formed from poly(*N*,*N*-diethylacrylamide) (PDEA) and commercially available dextran as well as poly(ethylene glycol) are investigated. Furthermore, the effect of an ATPS on the thermoresponsive behaviour of PDEA is studied. A significant shift in cloud point temperature of PDEA in the ATPS compared to pure aqueous PDEA solutions is observed. This effect on thermoresponsive behavior will lead to new pathways for water-based polymer systems for example in multicompartment hydrogels or biotechnology.

Introduction

In recent years, aqueous two-phase systems (ATPS) formed from polymer/polymer or polymer/salt mixtures have been of significant interest for polymer science.[1–3] Various applications for ATPS are discussed, mainly in the direction of biomedicine or food[4–6] as well as media for extraction, purification, and separation of proteins,[7] other biomolecules,[8] or metal ions.[9] ATPS formation is due to macroscopic liquid–liquid phase separation driven by two incompatible compounds in aqueous solution above a critical concentration.[10–12] Commonly, poly(ethylene glycol) (PEG) and dextran (Dex) are used to form an ATPS.[7,13] In the course of phase separation one polymer partitions into the upper phase and the other polymer into the lower phase. The phase separation depends on various factors, for example polymer concentration, pH, temperature as well as polymer molar mass.[14–18] ATPS are also directly related to water-in-water (w/w) emulsions, *i.e.* the dispersion of the two incompatible aqueous phases.[19–21] Again, PEG and Dex are used frequently for the formation of w/w emulsions.[22–24] These emulsions are also used for a variety of applications, *e.g.* in food,[25] microgel formation,[26] template for porous polymers[27] or multicompartment hydrogels.[28] The interface between both phases in ATPS is rather broad and has a low interfacial tension, at least in comparison to oil–water two-phase systems, which has a considerable effect on the demixing behaviour. Even more so, due to this feature w/w emulsions are commonly stabilised by nanoparticles in Pickering emulsion as small surfactants cannot cover the interface properly for stabilisation and neither phase has enough hydrophobic character for the surfactant to interact with.[29,30]

Stimuli-responsive polymers play an important role in polymer materials and the introduction of stimuli-response into ATPS and w/w emulsions is of significant interest. Recently, Georgiou and coworkers studied the temperature dependent phase behaviour of thermoresponsive poly(ethylene glycol) methacrylates in mixtures with Pluronic® F127 in phosphate buffered saline.[31] Shum and coworkers combined poly(*N*-isopropylacrylamide) and Dex to form viscoelastic networks.[32] An application of thermoresponsive polymers in ATPS is in molecular separation in order to retrieve the utilised polymers after the separation task is finished.[33,34] For example, Akashi and coworkers developed an ATPS based on poly(*N*-isopropylacrylamide) (PNIPAM) and poly(*N*-vinylisobutyramide) for improved partitioning of myoglobin.[35] Cao and coworkers designed an ATPS from two thermoresponsive polymers for the use of partitioning of antibiotics and subsequent recycling of the polymers.[36] In the case of w/w emulsions, stimuli-response can be introduced *via* the polymers themselves,[37] the underlying ATPS[38] or by the stabiliser.[39,40] Thermoresponsive w/w emulsions have been described by utilising thermoresponsive stabilisers, *e.g.* a reversible micellisation of a double hydrophilic block copolymer containing a thermoresponsive block or by employing thermoresponsive microgels.[39,40] Another stimulus that has been employed is pH, as introduced by stabilisers like linear polyelectrolytes,[41] pH responsive double hydrophilic block copolymers,[42] polysac-

[a]*School of Chemistry, University of Glasgow, Glasgow G12 8QQ, UK.*
E-mail: bernhard.schmidt@glasgow.ac.uk
[b]*Department of Chemistry, University of Warwick, Coventry, CV4 7AL, UK*

† Electronic supplementary information (ESI) available. See DOI: https://doi.org/10.1039/d3py00734k

charide-coated protein particles[43] or pH responsive microgels.[44] Also light has been used as a stimulus to break w/w emulsions.[45]

The effect of additives on the temperature-driven aggregation behaviour of thermoresponsive polymers has been studied frequently, *e.g. via* salt addition.[46,47] Also, the addition of PEG as a crowding agent to solutions of PNIPAM has been studied.[48] It was shown that the cloud point shifts with the addition of a crowding polymer. In a similar way, the effect of crowding on the thermoresponsive aggregate formation of poly(2-oxazoline)-based block copolymers was studied.[49] A commonly used thermoresponsive polymer is poly(*N*,*N*-diethylacrylamide) (PDEA).[50] It features a lower critical solution temperature (LCST) around 33 °C with a relatively sharp transition.[51,52] PDEA has been used in various studies, for example in multi-responsive micelles,[53] bioconjugates,[54] hydrogel actuators[55] or in supramolecular block copolymers.[56] PDEA with a broad range of molar masses can be synthesised *via* various polymerisation techniques including reversible addition–fragmentation chain transfer (RAFT) polymerisation, *e.g.* photo-iniferter (PI)-RAFT photopolymerisation.[57,58] Recently, PI-RAFT polymerisations under blue light were described[59] and in here visible light LEDs were utilised.

Herein, we describe the ATPS formation of PDEA with commercial Dex (40 kg mol^{-1}) or PEG (35 kg mol^{-1}) as well as the aqueous-three phase system (A3PS) comprising all three polymers in water (Scheme 1). Two PDEAs were synthesised *via* photo-initiated RAFT (PI-RAFT) polymerisation varying molar masses between 40 kg mol^{-1} and 55 kg mol^{-1}. Phase diagrams of the ATPS for PDEA/Dex and PDEA/PEG were assembled and partitioning of the polymers in different phases were analysed. Next, the thermoresponsive behaviour was investigated for each phase individually with respect to polymer concentration and ratio. Although the literature showed that ATPS can be formulated with thermoresponsive polymers, especially for the use in separation applications, the effect of an ATPS surrounding on the thermoresponsive behaviour itself has not been studied. Thus, we investigated the change of cloud points in an ATPS depending on phase composition. In contrast to the addition of crowding agents to change the thermoresponsive behaviour, the effect of a two-phase system is studied in here to enable the design of a thermoresponsive ATPS.

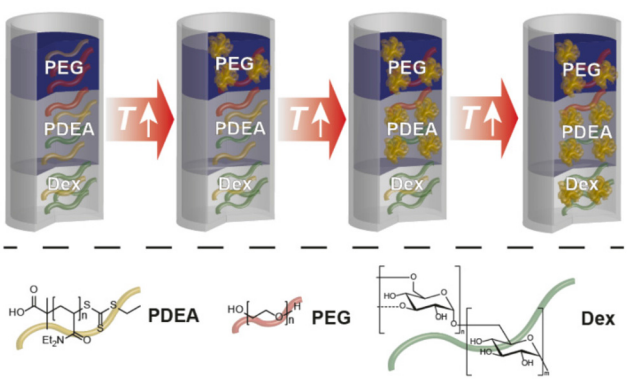

Scheme 1 Overview of the cloud point shift in ATPS of PDEA and Dex and utilised polymers (poly(*N*,*N*-diethylacrylamide) (PDEA, yellow); poly (ethylene glycol) (PEG, red); dextran (Dex, green)).

Experimental

Materials

Acetone (Fisher, analytical grade), dichloromethane (DCM, analytical grade, VWR), 2-bromisobutyric acid (98.5%, Sigma Aldrich), carbon disulfide (CS_2, 99%, Sigma-Aldrich), dextran (Dex, TCI, 40 kg mol^{-1}), *N*,*N*-diethylacrylamide (DEA, TCI, passed over a column of basic aluminium oxide), *N*,*N*-dimethyl formamide (DMF, SLS), ethanethiol (98%, Alfa Aesar), ethyl acetate (99.5%, VWR), *n*-hexane (95%, Sigma Aldrich), hydrochloric acid (conc., Fisher), Millipore water (obtained from an Sartorius Arium pro ultrapure water system), poly(ethylene glycol) (PEG, Sigma Aldrich, 35 kg mol^{-1}), potassium phosphate (Sigma Aldrich) and sodium sulfate (anhydrous, SLS) were used as received unless otherwise noted. 2-(((Ethylthio) carbonothioyl)thio)-2-methyl propanoic acid (EMP) was synthesised according to the literature.[60,61]

Analytical methods

^{1}H NMR spectra were recorded in deuterium oxide (D_2O, Aldrich) at ambient temperature at 400 MHz with a Bruker Ascend400. Size exclusion chromatography (SEC) of PDEA was conducted in THF at 35 °C using a column system with an Agilent PL Gel Guard Column (5 μm) and an Agilent PL Gel Mixed-D Column (5 μm) as well as an Agilent Infinity1260 II RID and calibration with poly(styrene) (PS) standards. Partition coefficients and mole fractions were determined *via* the concentration calculated from ^{1}H NMR spectra using DMF as internal standard according to eqn (S1)–(S4) (ESI†). Turbidimetry was performed with an Agilent Technologies Cary 3500 Multicell UV-Vis Spectrophotometer equipped air-cooled Peltier system and PS semi-micro cuvettes (light path of 10.00 mm) were used for measurements.

Exemplary PI-RAFT-polymerisation of DEA

Destabilised DEA (4.0 g, 31.5 mmol, 1575 eq.), EMP (4.5 mg, 0.02 mmol, 1.0 eq.), and DMF (4 mL) were mixed in a vial containing a stirring bar and sealed with a septum. The solution was bubbled with nitrogen for 30 min and the polymerisation was initiated using two visible light LEDs 20 cm apart (50 W Bridgelux BXRA-50C5300; λ > 410 nm, connected to a self-made circuit and cooling system). The polymerisation was stopped after 24 h. Subsequently, the polymer was dialysed against deionised water (Spectra/Por 3500 Da) for 3 days. Finally, the sample was freeze-dried and a slightly yellow solid (1.91 g, M_n = 54 800 g·mol^{-1}, $Đ$ = 1.30) was obtained.

Preparation of ATPS and phase diagram

PDEA (50 mg) was dissolved in deionised water (450 mg) to obtain a 10 wt% solution. A 10 wt% solution of Dex or PEG

was prepared in the same way. Afterwards both solutions were mixed to receive a 5.0 wt%/5.0 wt% mixture. Subsequently, the solution was equilibrated at ambient temperature in order to demix, investigated and diluted (100 mg of deionised water each cycle). The process was repeated, until no phase separation was observed. The average weight concentration between the last addition and the second to last addition was recorded as the data point for the binodal curve. All other concentration combinations (1 wt%/9 wt%, 3 wt%/7 w%, 7 wt%/3 wt%, 13.5 wt%/1.5 wt%) were analysed in a similar way.

Measurement of cloud points

The cloud points of each individual phase for different mixtures were measured subsequently after complete phase separation. Initially, the uppermost phases were meticulously collected and subjected to precise measurements, followed by subsequent measurements of bottom phases for ATPS. In the case of A3PS the middle phase was measured in addition. Heating and cooling cycles between 10 and 60 °C were performed with a temperature gradient of 2 °C min^{-1} at λ = 520 nm for each sample. All the data were obtained using Cary UV Workstation software. The cloud point was obtained at a transmittance of 50%.

Results and discussion

Synthesis of various poly(*N*,*N*-diethylacrylamide)s *via* PI-RAFT polymerisation

In order to form ATPS, PDEA with two different molar mass were synthesised *via* PI-RAFT polymerisation (Fig. S1†). EMP was used as photoinitiator in DMF *via* visible light. Conversions between 60 and 81% were obtained after 24 h as determined by ^{1}H NMR. Furthermore, the purified polymer samples were analysed *via* ^{1}H NMR (Fig. S1†). SEC analysis in THF against PS standards indicated molar mass values of M_n = 40 000 g mol^{-1} and M_n = 54 800 g mol^{-1} and dispersity indices of $Đ$ = 1.26 and $Đ$ = 1.30, respectively (Fig. S2 and Table S1†).

ATPS of PDEA and Dex or PEG

At first, the phase separation behaviour of PDEA and Dex or PEG in water was investigated. Phase diagrams were assembled for two polymer systems $PDEA_{55k}$/Dex and $PDEA_{55k}$/PEG (Fig. 1).

The ATPS phase diagram was assembled by checking the formation of two phases *vs.* one phase at a given weight ratio of polymers and overall polymer concentration. At first, start solutions with a total of 10 wt% polymer concentration (except 15 wt% for high PDEA content) and various weight ratios (1/9, 3/7, 5/5, 7/3, 13.5/1.5 PDEA to Dex or PEG) were prepared (Fig. 1b and c). The solutions were mixed and kept still to equilibrate at ambient temperature. Next, the mixture was inspected for two-phase formation, and diluted in case two phases were observed. This process was repeated until no two-phase formation was observed and the corresponding concentration noted. The average concentration between the last concentration with visible phase separation and the first concentration with no phase separation, was used as a data point for the binodal. The binodal is the line separating the one- and two-phase area in the phase diagram, which allows to deduce a valid concentration and ratio of polymers for phase separation (Fig. 1a). The binodal is not only the line separating the one- and two-phase region but also gives the composition of each phase in equilibrium. At any position in the two-phase region of the phase diagram, demixing will occur and a tie line can be constructed. The composition of each phase equals the polymer composition *x*- and *y*-value in the phase diagram at the two intersections of tie line and binodal. Overall, a phase separation was observed with concentrations as low as 3.0/3.0 wt% for PDEA/Dex and PDEA/PEG, which gives the minimum total polymer concentration to form an ATPS for these polymers at 6 wt%. The two-phase area of PDEA/PEG is slightly larger than PDEA/Dex.

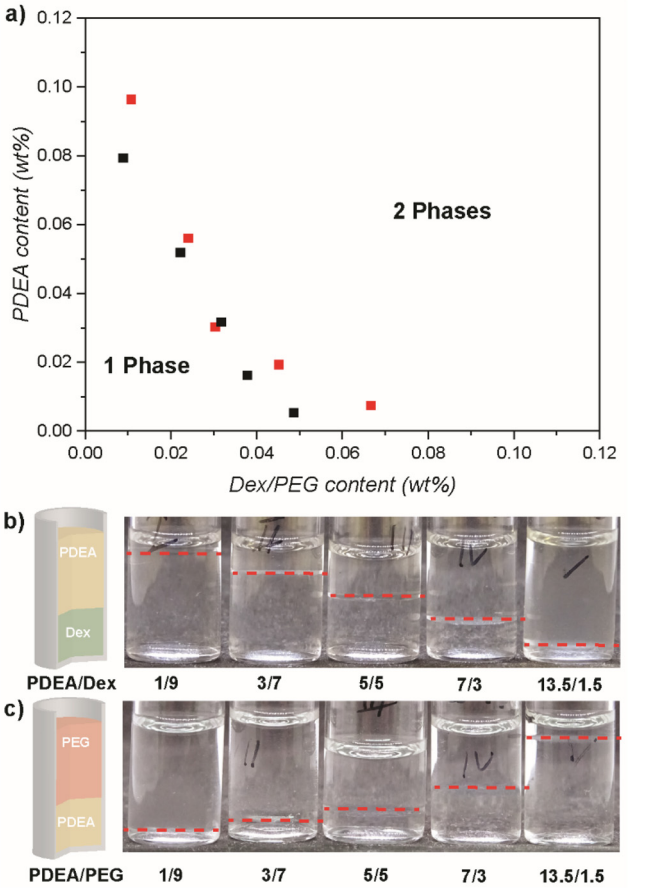

Fig. 1 (a) Phase diagrams of the ATPS for $PDEA_{55k}$ and Dex (black squares for the binodal) as well as $PDEA_{55k}$ and PEG (red squares for the binodal). (b) ATPS composed of $PDEA_{55k}$ and Dex at various ratios (from left to right PDEA/Dex: 1 wt%/9 wt%, 3 wt%/7 w%, 5 wt%/5 wt%, 7 wt%/3 wt%, 13.5 wt%/1.5 wt%). (c) ATPS composed of $PDEA_{55k}$ and PEG at various ratios (from left to right PDEA/PEG: 1 wt%/9 wt%, 3 wt%/7 w%, 5 wt%/5 wt%, 7 wt%/3wt%, 13.5 wt%/1.5 wt%).

To evaluate the demixing process of the individual polymer types in the ATPS and identify the location of the polymer

types in the phases, their partitioning was investigated. ^{1}H NMR of each phase was analysed (Fig. S3 and S4†) employing DMF as internal standard. For the PDEA$_{55k}$/Dex system, PDEA was enriched in the upper phase and Dex was enriched in the lower phase of the ATPS (Fig. 2a). As expected, in each phase a residual amount of the opposite polymer was present. At a starting concentration of 5/5 wt%, the partition coefficients (Table S2 and eqn (S1)†) for the ATPS of PDEA$_{55k}$ and Dex were 9.45 for PDEA and 0.11 for Dex in the upper phase as well as 0.11 and 3.38 in the lower phase, respectively. Overall, Dex prefers the bottom phase (Tables S2 and S3†), while the Dex concentration is rather low in the PDEA enriched phase. The enrichment of Dex in the bottom phase is the strongest for a composition of 7 : 3 PDEA/Dex (Fig. S5†). For PDEA, the highest enrichment was observed for the composition of 3 : 7 PDEA/Dex by a large margin. In the bottom phase, PDEA is present only in minor quantities (Fig. S5†).

In a similar way, the ATPS of PDEA$_{55k}$ with PEG was analysed (Table S4†). For the PDEA/PEG system, PEG was enriched in the upper phase and PDEA was enriched in the lower phase of the ATPS (Fig. 2b). At a starting concentration of 5/5 wt%, partition coefficients for the ATPS of PDEA$_{55k}$ and PEG were 0.18 for PDEA and 3.93 for PEG in the upper phase as well as 5.41 and 0.25 in the lower phase, respectively. Overall, PEG prefers the top phase, albeit the concentration of PEG in the PDEA phase is still quite high (Tables S4, S5 and Fig. S5†). PDEA enriches in the bottom phase but still significant amounts are present in the top phase as well. The highest enrichment of PDEA is observed for a composition of 7 : 3 PDEA/PEG (Fig. S5†).

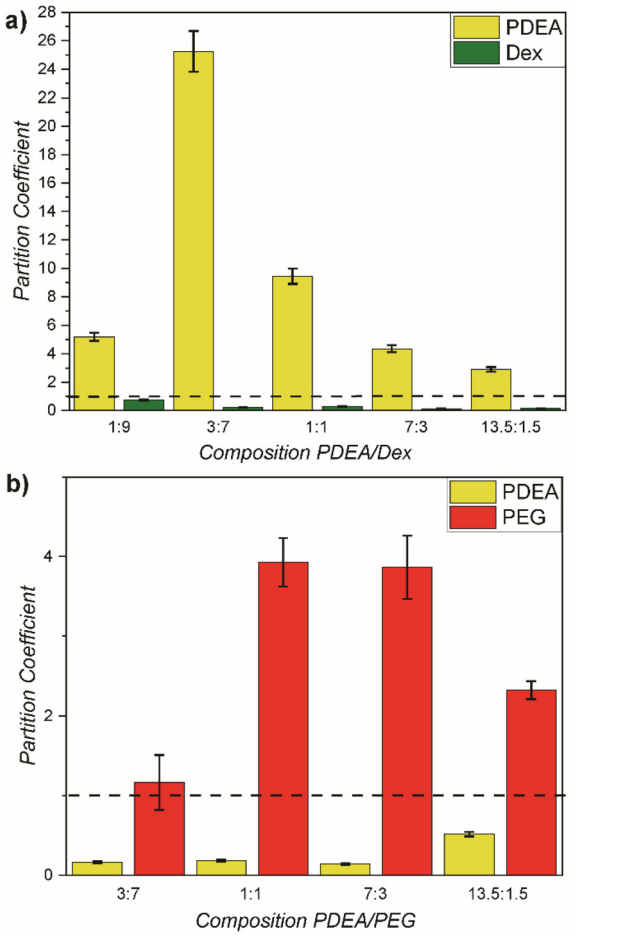

Fig. 2 Partitioning of polymers in ATPS (values above 1, *i.e.* the dotted line, mean enrichment in top phase; values below 1 mean enrichment in bottom phase): (a) partitioning of PDEA$_{55k}$ and Dex in ATPS of various and (b) partitioning of PDEA$_{55k}$ and PEG in ATPS of various composition.

Comparison of the PDEA/Dex and PDEA/PEG ATPS shows a significant difference. First of all, in the case of PDEA/Dex the Dex enriched phase is at the bottom meaning it is the denser phase, while for PDEA/PEG, the PDEA enriched phase is at the bottom. The partition coefficients show a strong partitioning of PDEA in the PDEA/PEG system as well as segregation to a larger extent in the PDEA/Dex system. Dex and PEG have a similar partitioning between enriched and depleted phase in their respective systems. The partition coefficients are related to the phase diagram *via* the binodal. As mentioned before, the binodal gives the equilibrium concentration for each polymer for a defined starting concentration *via* the tie line. As such, partition coefficients – being related to equilibrium concentration – are connected to the binodal in the phase diagram.

Thermoresponse in ATPS of PDEA and Dex

After analysing the phase behaviour of the ATPS of PDEA and Dex, we investigated the thermoresponse of PDEA in the ATPS. Optical inspection showed a difference in cloud point between the reference, the top phase and the bottom phase (Fig. 3a). Turbidimetry confirmed the observations. We prepared ATPS with three different ratios to study the effect of composition on the cloud point. In the ATPS the cloud point shifts to lower temperatures (Fig. 3 and Table S6†). For PDEA$_{40k}$/Dex this meant a shift from 41.2 to 40.5 °C for the top phase and 35.5 °C for the bottom phase in a 5/5 wt% ATPS. For the mixture PDEA$_{40k}$/Dex 3 : 7 a shift from 40.9 to 34.8 °C for the top phase and 36.9 °C for the bottom phase was observed. The mixture PDEA$_{40k}$/Dex 7 : 3 showed changes from 41.5 to 38.7 °C for the top phase and 37.7 °C for the bottom phase. Similar results were obtained for PDEA$_{55k}$ (Fig. S6†).

The difference in the cloud point is connected to the investigated phase, our results indicate that the PDEA enriched phase has a cloud point closer to the reference. Reference measurements were performed in water with the same overall PDEA concentration as in the ATPS. Commonly the cloud point is a function of polymer concentration as increasing the polymer concentration in solution leads to a decrease in the cloud point temperature due to thermodynamic interactions between the polymer chains. The thermodynamic partitioning of the thermoresponsive polymer significantly impacts the concentration distribution within the respective phases, thereby leading to a shift in the cloud point. Furthermore, in the context of the ATPS, the introduction of an additional polymer also exerts an influence. Notably, distinct disparities are observed in the turbidimetry curve shapes between the

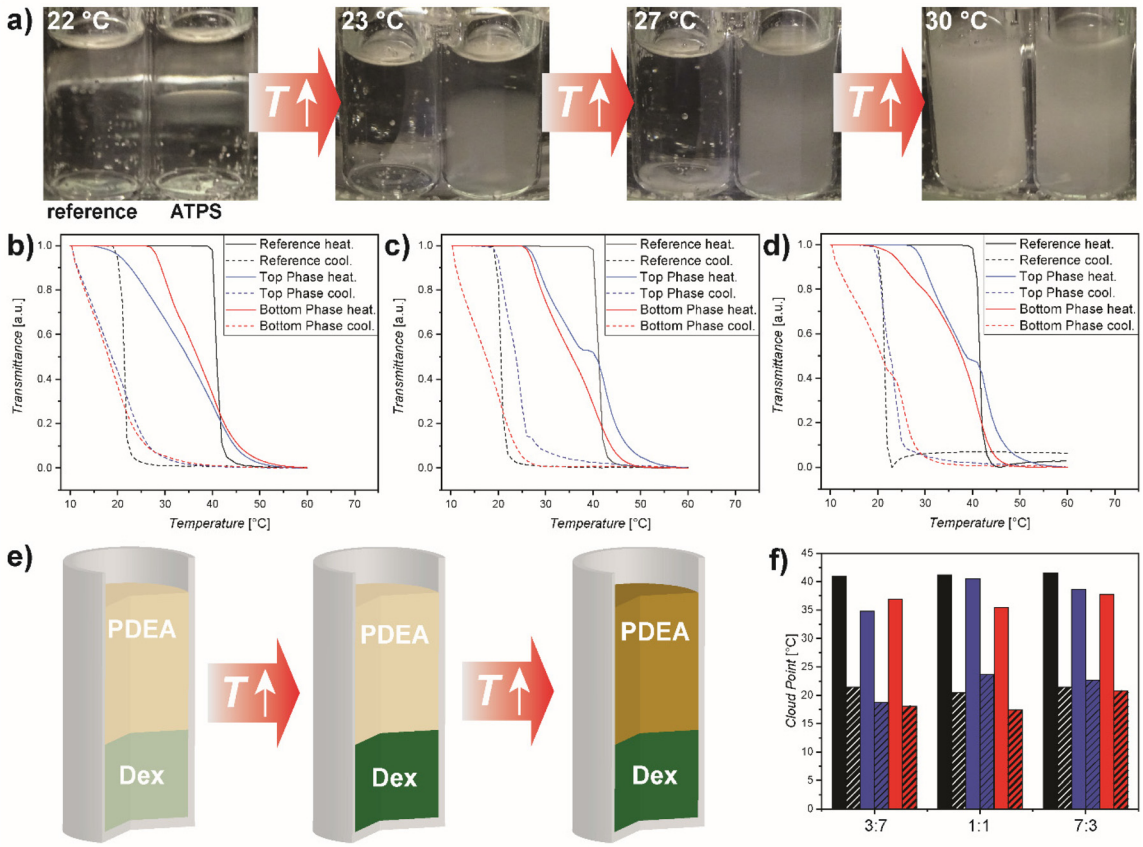

Fig. 3 Thermoresponse of PDEA/Dex ATPS: (a) photographs of ATPS formed from $PDEA_{40k}$/Dex 5 wt%/5 wt% during heating (reference $PDEA_{40k}$ in water at 5 wt%, heating rate at 0.2 °C min^{-1}), (b) turbidimetry results of $PDEA_{40k}$/Dex 3 wt%/7 wt% (reference $PDEA_{40k}$ in water at 3 wt%, heating rate at 2 °C min^{-1}), (c) turbidimetry results of $PDEA_{40k}$/Dex 5 wt%/5 wt% (reference $PDEA_{40k}$ in water at 5 wt%, heating rate at 2 °C min^{-1}), (d) turbidimetry results of $PDEA_{40k}$/Dex 7 wt%/3 wt% (reference $PDEA_{40k}$ in water at 7 wt%, heating rate at 2 °C min^{-1}), (e) schematic of ATPS clouding and (f) cloud points for various compositions of $PDEA_{40k}$/Dex ATPS (solid: heating, shaded: cooling; black: reference, blue: top phase, red: bottom phase).

reference system and the ATPS configuration. While the reference has a rather sharp transition in the range of 1 °C, the change in transmittance proceeds over a broader temperature interval of 5–20 °C. This effect might be due to the presence of hydrophilic Dex in both phases, which interferes with the coil to globule transition of PDEA. As described before, molecular crowding has a significant effect on thermoresponsive behaviour,[48] which is a factor the ATPS introduces due to the partitioning of both polymers in both phases.

Interestingly, in all cases – ATPS and reference – a strong hysteresis of the thermoresponsive behaviour between heating and cooling was observed. Initially, we hypothesised that this effect might be attributed to the high overall polymer concentration, considering the observed hysteresis even in the Dex-enriched phase. To gain deeper insights, additional turbidimetric measurements were conducted using low-concentration PDEA (Fig. S7†). Remarkably, a significant hysteresis was still evident at low concentrations (cloud point: 42.0 °C during heating and 22.4 °C during cooling), indicating that concentration does not play a major role in the observed hysteresis of the investigated PDEA system. Furthermore, the cloud point measurements in the diluted PDEA solution revealed a contrasting behaviour, where dilution led to an upward shift of the cloud point to higher temperatures, contrary to the observations in the ATPS system. We further noticed a significant dependence on heating/cooling rate (Fig. S7†), showing that the hysteresis is much less pronounced for slower temperature ramps. Furthermore, the cloud point shifts with slower temperature ramp as well (Fig. 3a and c), while the overall trend is preserved.

Consequently, we posit that polymer–polymer interactions exert an influential role on the cloud point as well as heating/cooling rate, while concentration merely exerts a minor influence on the observed cloud points. It is obvious that the complex interrelationship among molecular interactions, concentration, and thermodynamic factors necessitates extensive investigation to gain a comprehensive understanding of the underlying mechanisms governing the observed hysteresis and cloud point behaviour in the studied PDEA system.

Thermoresponse in A3PS of PDEA, Dex and PEG

One special feature of aqueous multi-phase systems *versus* amphiphilic systems is the option to obtain more than two phases. Encouraged by our results from the PDEA/Dex ATPS, it

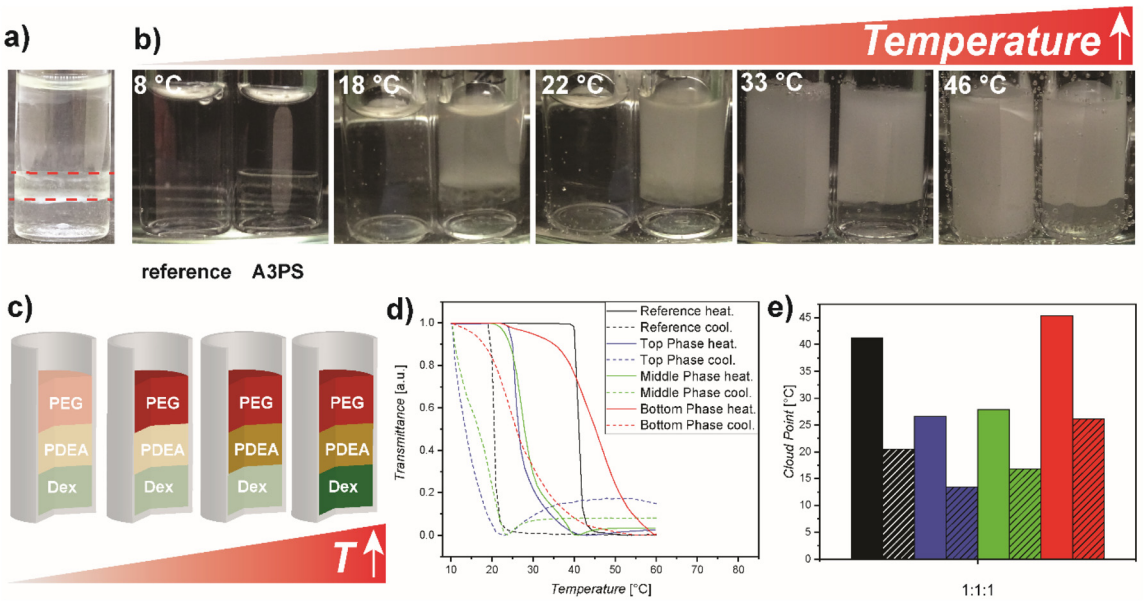

Fig. 4 Thermoresponse of PDEA/Dex/PEG A3PS: (a) photograph of the $PDEA_{40k}$/Dex/PEG A3PS at 5 wt%/5 wt%/5 wt%, (b) photographs of A3PS formed from $PDEA_{40k}$/Dex/PEG at 5 wt%/5 wt%/5 wt% during heating (reference $PDEA_{40k}$ in water at 5 wt%, heating rate at 0.2 °C min^{-1}), (c) schematic of A3PS clouding, (d) turbidimetry results of $PDEA_{40k}$/Dex/PEG 5 wt%/5 wt%/5 wt% (reference $PDEA_{40k}$ in water at 5 wt%, heating rate at 2 °C min^{-1}) and (e) cloud points for the A3PS of $PDEA_{40k}$/Dex/PEG (solid: heating, shaded: cooling; black: reference, blue: top phase, green: middle phase, red: bottom phase).

was decided to investigate thermoresponse in an A3PS from PDEA/Dex/PEG (Fig. 4a). Therefore, an A3PS PDEA/Dex/PEG with a concentration of 5 wt% for each polymer type was prepared. Analysis of the phase compositions showed enrichment of PEG in the top phase, enrichment of PDEA in middle phase and enrichment of Dex in the bottom phase (Fig. S8 and Tables S7, S8†), as shown by calculation of partition coefficients and mole fractions (eqn (S3) and (S4)). PDEA is predominantly present in the middle phase but significant amount is present in the top phase as well. In the bottom phase, PDEA has only low concentration. PEG is enriched in the top phase and only minor amounts of PEG are present in the other two phases. Dex is the majority component in the bottom phase but significant amounts are present in the middle phase as well. In the top phase, Dex is only present in very small amounts.

Similar to the ATPS of PDEA and Dex, a shift in the cloud point was observed optically, as well as differences in the cloud point between the individual phases (Fig. 4b). In comparison to the reference, the cloud point shifted to lower temperatures in the top and middle phase significantly. A shift of 10–15 °C was observed (Table S9†). The cloud point shifted around 4 °C to higher temperatures for the bottom phase. Apparently, the addition of PEG has a stronger effect on the thermoresponsive behaviour than Dex. This strengthened effect could be due to a change in hydrogen bonding, *i.e.* Dex is a hydrogen bond donor with free hydroxyl groups and PEG is a hydrogen bond acceptor. Given the hydrogen bond acceptor properties of PDEA, it can be postulated that Dex plays a role in stabilising PDEA within the solution by serving as a mediator between water and the thermoresponsive polymer. On the other hand, PEG induces globule formation due to the absence of significant interactions. A similar effect was observed for one-phase mixtures of PEG and PNIPAM.[48]

Another factor is polymer concentration in the individual phases, PDEA has the highest concentration in the middle phase followed by the top phase. In the bottom phase PDEA has the lowest concentration. Compared to the ATPS a more significant change in cloud point was observed for the top and middle phase, although the PEG concentration is rather low in the middle phase. Apparently, a small amount of PEG can already shift the cloud point significantly. Similar to the ATPS, a strong hysteresis of the thermoresponsive behaviour was observed for all phases.

Conclusions

ATPS are a major topic in current research on hydrophilic polymers. In parallel, extensive focus has been placed on stimuli-responsive polymers and thermoresponsive polymers. This study combines both aspects, as we demonstrate the modulation of the thermoresponsive behaviour of PDEA when introduced into a PDEA/Dex ATPS. Furthermore, we show that the thermoresponsive behaviour is altered by phase composition. A unique feature of aqueous multi-phase systems was exploited as well, namely the formation of more than two phases, *e.g.* an A3PS. Notably, the impact on cloud points exhibited greater prominence in the PDEA/Dex/PEG A3PS compared to the ATPS, resulting in shifts of up to 15 °C. We believe these results

exemplify the capacity of aqueous multi-phase systems to finely tune the properties of hydrophilic polymers. In particular, the development of a model to predict thermoresponsive behaviour in multi-phase systems would be beneficial and will be addressed in future work. These thermoresponsive multi-phase systems present opportunities for applications in biotechnology, biomedicine, cosmetics, and food industries.

Author contributions

NB: Data collection, review and editing the draft. GY: Data collection, review and editing the draft. RB: Review and editing the draft, supervision. BS: Conceptualisation, data collection, writing original draft, supervision, funding acquisition.

Conflicts of interest

There are no conflicts to declare.

Acknowledgements

B.S. and N.B. acknowledge funding from EPSRC in the form of a DTG Studentship. B.S. and A.P. acknowledge funding the German Research Foundation (Grant No. SCHM 3282/3-1).

References

1 Y. Chao and H. C. Shum, *Chem. Soc. Rev.*, 2020, **49**, 114–142.
2 B. V. K. J. Schmidt, *Macromol. Chem. Phys.*, 2018, **219**, 1700494.
3 M. Iqbal, Y. Tao, S. Xie, Y. Zhu, D. Chen, X. Wang, L. Huang, D. Peng, A. Sattar, M. A. B. Shabbir, H. I. Hussain, S. Ahmed and Z. Yuan, *Biol. Proced. Online*, 2016, **18**, 18.
4 R. Haag and F. Kratz, *Angew. Chem., Int. Ed.*, 2006, **45**, 1198–1215.
5 J.-W. Rhim, H.-M. Park and C.-S. Ha, *Prog. Polym. Sci.*, 2013, **38**, 1629–1652.
6 M. Rito-Palomares, A. Negrete, E. Galindo and L. Serrano-Carreon, *J. Chromatogr. B: Biomed. Sci. Appl.*, 2000, **743**, 403–408.
7 J. A. Asenjo and B. A. Andrews, *J. Chromatogr. A*, 2011, **1218**, 8826–8835.
8 C. D. Keating, *Acc. Chem. Res.*, 2012, **45**, 2114–2124.
9 P. da Rocha Patrício, M. C. Mesquita, L. H. M. da Silva and M. C. H. da Silva, *J. Hazard. Mater.*, 2011, **193**, 311–318.
10 J. F. Pereira, M. G. Freire and J. A. Coutinho, *Fluid Phase Equilib.*, 2020, **505**, 112341.
11 P. Albertsson, *Biochem. Pharmacol.*, 1961, **5**, 351–358.
12 R. Hatti-Kaul, *Mol. Biotechnol.*, 2001, **19**, 269–277.
13 J. Ryden and P.-a. Albertsson, *J. Colloid Interface Sci.*, 1971, **37**, 219–222.
14 D. Forciniti, C. Hall and M.-R. Kula, *Fluid Phase Equilib.*, 1991, **61**, 243–262.
15 L. H. M. d. Silva, J. S. Coimbra and A. J. d. A. Meirelles, *J. Chem. Eng. Data*, 1997, **42**, 398–401.
16 W. J. Frith, *Adv. Colloid Interface Sci.*, 2010, **161**, 48–60.
17 A. P. Constantinou, A. Tall, Q. Li and T. K. Georgiou, *J. Polym. Sci.*, 2022, **60**, 188–198.
18 A. Plucinski, M. Pavlovic and B. V. K. J. Schmidt, *Macromolecules*, 2021, **54**, 5366–5375.
19 J. Esquena, *Curr. Opin. Colloid Interface Sci.*, 2016, **25**, 109–119.
20 T. Nicolai and B. Murray, *Food Hydrocolloids*, 2017, **68**, 157–163.
21 J. Esquena, *Curr. Opin. Food Sci.*, 2023, **51**, 101010.
22 H. Firoozmand, B. S. Murray and E. Dickinson, *Langmuir*, 2009, **25**, 1300–1305.
23 D. M. A. Buzza, P. D. Fletcher, T. K. Georgiou and N. Ghasdian, *Langmuir*, 2013, **29**, 14804–14814.
24 J. Zhang, J. Hwang, M. Antonietti and B. V. K. J. Schmidt, *Biomacromolecules*, 2018, **20**, 204–211.
25 P. Singh, B. Medronho, M. G. Miguel and J. Esquena, *Food Hydrocolloids*, 2018, **75**, 41–50.
26 S. Ma, J. Thiele, X. Liu, Y. Bai, C. Abell and W. T. S. Huck, *Small*, 2012, **8**, 2356–2360.
27 Y. Zhou, M. Zhu, Y. Sun, Y. Zhu and S. Zhang, *ACS Macro Lett.*, 2023, 302–307.
28 J. Zhang, B. Kumru and B. V. K. J. Schmidt, *Langmuir*, 2019, **35**, 11141–11149.
29 D. Forciniti, C. Hall and M. Kula, *J. Biotechnol.*, 1990, **16**, 279–296.
30 E. Scholten, J. E. Visser, L. M. Sagis and E. van der Linden, *Langmuir*, 2004, **20**, 2292–2297.
31 A. P. Constantinou, A. Tall, Q. Li and T. K. Georgiou, *J. Polym. Sci.*, 2022, **60**, 188–198.
32 H. Cui, Y. Zhang, Y. Shen, S. Zhu, J. Tian, Q. Li, Y. Shen, S. Liu, Y. Cao and H. C. Shum, *Adv. Mater.*, 2022, **34**, 2205649.
33 H. Musarurwa and N. T. Tavengwa, *Microchem. J.*, 2022, **179**, 107554.
34 Y. Zhang, H. Zhang, D. He, X. Cao and J. Wan, *Process Biochem.*, 2020, **99**, 254–264.
35 A. Kishida, Y. Kikunaga and M. Akashi, *J. Appl. Polym. Sci.*, 1999, **73**, 2545–2548.
36 D. Hou and X. Cao, *J. Chromatogr. A*, 2014, **1349**, 30–36.
37 J. Chen, J. Guo, X. Yang and T. Nicolai, *Food Hydrocolloids*, 2021, **118**, 106763.
38 M. Pavlovic, M. Antonietti, B. V. K. J. Schmidt and L. Zeininger, *J. Colloid Interface Sci.*, 2020, **575**, 88–95.
39 T. Merland, L. Waldmann, O. Guignard, M.-C. Tatry, A.-L. Wirotius, V. Lapeyre, P. Garrigue, T. Nicolai, L. Benyahia and V. Ravaine, *J. Colloid Interface Sci.*, 2022, **608**, 1191–1201.
40 M. Pavlovic, A. Plucinski, L. Zeininger and B. V. K. J. Schmidt, *Chem. Commun.*, 2020, **56**, 6814–6817.
41 L. Tea, T. Nicolai and F. Renou, *Langmuir*, 2019, **35**, 9029–9036.

42 A. Plucinski and B. V. K. J. Schmidt, *Polym. Chem.*, 2022, **13**, 4170–4177.
43 R. A. de Freitas, T. Nicolai, C. Chassenieux and L. Benyahia, *Langmuir*, 2016, **32**, 1227–1232.
44 B. T. Nguyen, W. Wang, B. R. Saunders, L. Benyahia and T. Nicolai, *Langmuir*, 2015, **31**, 3605–3611.
45 J. Zhang, B. D. Frank, B. Kumru and B. V. K. J. Schmidt, *Macromol. Rapid Commun.*, 2021, **42**, 2000433.
46 H. Du, R. Wickramasinghe and X. Qian, *J. Phys. Chem. B*, 2010, **114**, 16594–16604.
47 Y. Zhang, S. Furyk, D. E. Bergbreiter and P. S. Cremer, *J. Am. Chem. Soc.*, 2005, **127**, 14505–14510.
48 K. Sakota, D. Tabata and H. Sekiya, *J. Phys. Chem. B*, 2015, **119**, 10334–10340.
49 D. A. Estabrook, J. O. Chapman, S.-T. Yen, H. H. Lin, E. T. Ng, L. Zhu, H. L. van de Wouw, O. Campàs and E. M. Sletten, *J. Am. Chem. Soc.*, 2022, **144**, 16792–16798.
50 G. Delaittre, J. Rieger and B. Charleux, *Macromolecules*, 2011, **44**, 462–470.
51 I. Idziak, D. Avoce, D. Lessard, D. Gravel and X. X. Zhu, *Macromolecules*, 1999, **32**, 1260–1263.
52 K. Zhou, Y. Lu, J. Li, L. Shen, G. Zhang, Z. Xie and C. Wu, *Macromolecules*, 2008, **41**, 8927–8931.
53 X. André, M. Zhang and A. H. E. Müller, *Macromol. Rapid Commun.*, 2005, **26**, 558–563.
54 G. Kasza, T. Stumphauser, M. Bisztrán, G. Szarka, I. Hegedüs, E. Nagy and B. Iván, *Polymers*, 2021, **13**, 987.
55 X. Kong, Y. Li, W. Xu, H. Liang, Z. Xue, Y. Niu, M. Pang and C. Ren, *Macromol. Rapid Commun.*, 2021, **42**, 2100416.
56 B. V. K. J. Schmidt, M. Hetzer, H. Ritter and C. Barner-Kowollik, *Macromolecules*, 2013, **46**, 1054–1065.
57 R. N. Carmean, T. E. Becker, M. B. Sims and B. S. Sumerlin, *Chem*, 2017, **2**, 93–101.
58 A. Plucinski, M. Pavlovic, M. Clarke, D. Bhella and B. V. K. J. Schmidt, *Macromol. Rapid Commun.*, 2022, **43**, 2100656.
59 R. W. Hughes, M. E. Lott, J. I. Bowman and B. S. Sumerlin, *ACS Macro Lett.*, 2023, **12**, 14–19.
60 B. V. K. J. Schmidt, M. Hetzer, H. Ritter and C. Barner-Kowollik, *Macromolecules*, 2011, **44**, 7220–7232.
61 J. Skey and R. K. O'Reilly, *Chem. Commun.*, 2008, 4183–4185.